Nuclear Magnetic Resonance in the Paramagnetic States of MnO, α-MnS, and α-MnSe†

E. D. JONES
Sandia Laboratory, Albuquerque, New Mexico
(Received 6 June 1966)

The Mn^{55} and Se^{77} NMR have been observed in the paramagnetic states of the antiferromagnetic compounds MnO, α-MnS, and α-MnSe. The Mn^{55} and Se^{77} NMR frequency shifts were found to be temperature-dependent and proportional to the magnetic susceptibility. From an analysis of the NMR frequency shift and magnetic-susceptibility data, the following hyperfine coupling constants were determined: $A^{55}(\text{MnO}) = -(81.5\pm2.5)\times10^{-4}$ cm^{-1}, $A^{55}(\alpha\text{-MnS}) = -(71.8\pm5.3)\times10^{-4}$ cm^{-1}, $A^{55}(\alpha\text{-MnSe}) = -(67.0\pm4.5)\times10^{-4}$ cm^{-1} and $A^{77}(\alpha\text{-MnSe}) = +(7.2\pm0.6)\times10^{-4}$ cm^{-1}. Additional information regarding the Néel temperatures of α-MnS and α-MnSe was obtained by studying the temperature dependence of the Mn^{55} NMR intensity with the result $T_N(\alpha\text{-MnS}) = (147\pm1)$°K and $T_N(\alpha\text{-MnSe}) \simeq 150$°K. The experimental Mn^{55} and Se^{77} NMR linewidths were found to be in agreement with predictions based upon the theory of exchange-narrowed hyperfine-broadened NMR linewidths in paramagnetic insulators.

1. INTRODUCTION

NUCLEAR magnetic resonance (NMR) techniques in paramagnetic media provide information about, among other things, the sign and magnitude of the hyperfine interactions present in these materials. The hyperfine interaction experienced by a given nuclear species usually can be determined because of a linear relationship between the NMR frequency shift $\delta\nu/\nu$ (arising from the hyperfine interaction in question) and the paramagnetic susceptibility χ of the sample. However, the observation of the NMR of a nucleus of a paramagnetic ion may be difficult since the principal contribution to the NMR linewidth δH is believed to be due to the hyperfine interaction itself, which can be quite large. Thus, because of a large hyperfine interaction, the resulting NMR linewidth δH may be too broad to be observable. For example, applying the theory[1] of exchange-narrowed hyperfine-broadened NMR in paramagnetic insulators to MnF_2 indicates that the Mn^{55} NMR linewidth $\delta H^{55} \simeq 700$ Oe in the paramagnetic state and hence could account for the failure, thus far, to observe this particular Mn^{55} NMR.

A knowledge of the hyperfine interactions in magnetically dense materials such as MnO, α-MnS and α-MnSe can be used to study the questions concerning the origins of these hyperfine interactions. For example, of current interest is the question regarding contributions to the hyperfine interaction which are dependent upon the spin state of neighboring magnetic spins, i.e., is there a change in the magnitude of the hyperfine interaction, other than dipolar, upon transforming from a paramagnetic (spin-disordered) to an antiferromagnetic (spin-ordered) state? Such questions, of course, cannot be answered until the experimental data have been collected and comparisons have been made. Values for hyperfine interactions in magnetically ordered materials have been measured in a variety of compounds,[2] but these same hyperfine interactions, in general, have not been measured in the paramagnetic states, presumably because of the NMR linewidth problem discussed above.

Only a few NMR measurements of the nucleus of a magnetic ion have been performed in the paramagnetic state of magnetic insulators. Shulman[3] made the first such observation for the Co^{59} NMR in the paramagnetic states of CoO and $KCoF_3$. In this paper we wish to report the results and interpretations of the Mn^{55} and Se^{77} NMR in the paramagnetic states of MnO, α-MnS and α-MnSe. Preliminary data regarding the NMR in the paramagnetic states of MnO[4] and α-MnSe[5] have been reported. Shulman's[3] Co^{59} and our Mn^{55} NMR data represent the only measurements, to date, of the NMR of a magnetic ion in a paramagnetic insulator.

The experimental apparatus and technique used to observe the Mn^{55} and Se^{77} NMR in MnO, α-MnS and α-MnSe are discussed in Sec. 2. The origins, results and analysis of the NMR frequency shift data are presented in Sec. 3. Section 4 contains the theoretical and experimental analysis of the contributions to the NMR line shapes and linewidths in the paramagnetic states of MnO, α-MnS and α-MnSe. It is also shown in Sec. 4 that the theory of exchange-narrowed hyperfine-broadened NMR linewidths, as developed by Moriya,[1] is in essential agreement with experimental observations. Section 5 gives a summary of the NMR data presented in this paper.

2. EXPERIMENTAL

The Mn^{55} and Se^{77} NMR were observed in powdered and polycrystalline samples of MnO, α-MnS, and α-MnSe, using a variable-frequency induction NMR spectrometer and a conventional 12-in. electromagnet.

† Part of this work was performed by the author at Bell Telephone Laboratories, Murray Hill, New Jersey and the remaining work was supported by the U. S. Atomic Energy Commission.

[1] T. Moriya, Progr. Theoret. Phys. (Kyoto) 16, 641 (1956).

[2] The reader is referred to the review articles on NMR in magnetically ordered systems by V. Jaccarino and A. Portis, in *Magnetism*, edited by H. Suhl and G. Rado (Academic Press Inc., New York, 1965), Vol. IIA.

[3] R. G. Shulman, Phys. Rev. Letters 2, 459 (1959).

[4] E. D. Jones, J. Appl. Phys. 36, 919 (1965).

[5] E. D. Jones, Phys. Letters 18, 98 (1965).

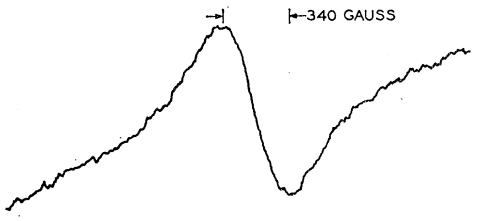

FIG. 1. A tracing of a room-temperature Mn^{55} NMR in MnO.

Sample temperatures between 130 and 350°K were achieved by use of a Varian V-4540 variable temperature-control unit which was calibrated against a copper-constantan thermocouple. The Mn^{55} NMR frequency shift measurements were made at various fixed frequencies ranging from 8 to 16 Mc/sec, by measuring the magnetic field for which the Mn^{55} NMR occurred with respect to a saturated solution of $KMnO_4$. The Se^{77} NMR frequency-shift measurements in α-MnSe were made with respect to the Al^{27} NMR in a saturated solution of $Al_2(SO_4)_3$. The maximum available modulation field amplitude was about 40 Oe at 20 cps. The MnO, α-MnS, and α-MnSe samples were verified to have the NaCl structure by standard x-ray powder-pattern techniques.

Magnetic-susceptibility measurements were performed on MnO, α-MnS, and α-MnSe samples using a pendulum magnetometer and a magnetic field of 15.3 kOe. Our susceptibility measurements on these samples were found to be in agreement with previously reported data (see Sec. 3).

A tracing of a room-temperature Mn^{55} NMR in MnO is shown in Fig. 1. This is an example of the best signal-to-noise ratio obtained for these NMR data. The absorption derivative peak-to-peak NMR linewidth $\delta H \simeq 340$ Oe, within experimental error, was found to be field-independent between 8 and 16 kOe thereby indicating negligible demagnetization broadening of the Mn^{55} NMR. Similar results were obtained for the Mn^{55} NMR in α-MnS, α-MnSe and for the Se^{77} NMR in α-MnSe.

3. NMR FREQUENCY SHIFTS IN THE PARAMAGNETIC STATES OF MnO, α-MnS AND α-MnSe

Above their Neél temperatures, MnO, α-MnS and α-MnSe have the cubic NaCl-type crystal structure which removes complications of the use of nonsingle-crystal samples for the NMR data. Furthermore, because Mn^{2+} is a S-state ion and is located at a site with cubic symmetry, there are no anisotropic hyperfine, magnetic dipolar hyperfine or nuclear electric quadrupolar interactions which will contribute to the Mn^{55} NMR frequency shift.

Thus for a Mn^{55} nucleus in the paramagnetic state of MnO, α-MnS or α-MnSe, the nuclear spin Hamiltonian, which contains only one hyperfine interaction (resulting from core-polarization of the inner s-shell electrons by the outer 3-d electrons) may be written as

$$\mathcal{H}^{55}=\gamma^{55}\hbar\mathbf{I}\cdot\mathbf{H}_0+A^{55}\mathbf{I}\cdot\langle\mathbf{S}\rangle, \tag{3.1}$$

where γ^{55} is the Mn^{55} nuclear gryomagnetic ratio, I is the nuclear spin, H_0 is the applied magnetic field, A^{55} is the nuclear hyperfine interaction resulting from core-polarization and $\langle S\rangle$ is the time-averaged electron spin polarization per Mn^{2+} ion. For purposes of analysis, A^{55} is assumed to be temperature-independent in the range of 130–300°K. The Mn^{55} NMR frequency shift $a^{55}=(\delta\nu/\nu)^{55}$ is thus found from Eq. (3.1) to be

$$a^{55}(T)=(Ng\beta)^{-1}(A^{55}/\gamma^{55}\hbar)\chi_d(T), \tag{3.2}$$

where N is Avogadro's number, $g\simeq 2$ is the Mn^{2+} electronic g value, β is the Bohr magneton and $\chi_d(T)$ is the temperature-dependent Mn^{2+} spin susceptibility expressed in emu/mole. In deriving Eq. (3.2), contributions to $a^{55}(T)$ from diamagnetic-susceptibility or demagnetization-field effects have been ignored. The reason for neglect of the diamagnetic shift is two-fold: (1) the diamagnetic susceptibility $\chi_{\text{dia}}\simeq -30\times10^{-6}$ emu/mole and is small compared with $\chi_d(300°K)\simeq 5000\times10^{-6}$ emu/mole, and (2) the Mn^{55} NMR frequency shifts were made with respect to a $KMnO_4$ reference solution and thus the difference in the diamagnetic shift between reference and sample NMR frequencies should be negligible.

An estimate of the demagnetization field contribution to the Mn^{55} NMR frequency shift was made in the following manner. We first assume (with no experimental justification) that the powder particles are somewhat spherical in shape, and also that because of the cubic symmetry of the lattice, there will be no demagnetization-field corrections to the applied magnetic field from the particles themselves. Thus, the only contribution which we can expect will be from the over-all shape of the sample. An estimate for this demagnetization field correction is difficult to make since the volume density of the samples varied from sample to sample. Therefore, the following experiment was performed in order to determine an approximate value of the demagnetization field shift of the NMR frequency. Finely powdered cadmium metal, about 1% by weight, was mixed into the MnO sample. The Cd^{113} NMR spectrum of the Cd-MnO mixture was then compared to the pure Cd^{113} NMR with the result that at 16 kOe, the maximum field shift ΔH which could be assigned to the Cd^{113} NMR in the Cd-MnO mixture was $\Delta H\simeq 2$ G. The uncertainties involved in the actual measurements of the value of the resonance field are ± 10 G for the Mn^{55} NMR and about ± 2 G for the Se^{77} NMR. Therefore, we feel justified in neglecting demagnetization field corrections to the NMR frequency shifts.

In the same manner that Eq. (3.2) was derived for the Mn^{55} NMR frequency shift, one can write an

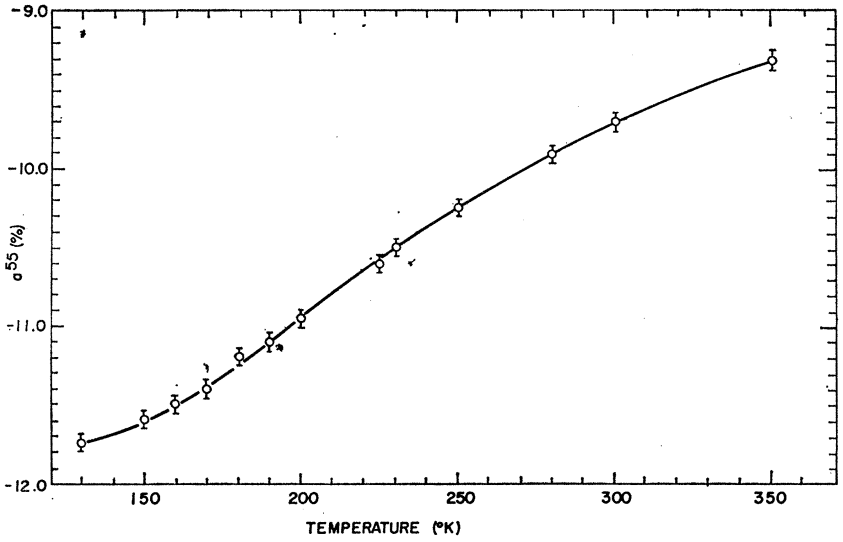

FIG. 2. The temperature dependence of the Mn^{55} NMR frequency shift a^{55} in the paramagnetic state of MnO.

expression for the Se^{77} NMR frequency shift $a^{77}(T)$ as

$$a^{77}(T)=(Ng\beta)^{-1}(6A^{77}/\gamma^{77}\hbar)\chi_d(T), \qquad (3.3)$$

where the factor of 6 arises from the six neighboring Mn^{2+} ions, each contributing a transferred hyperfine interaction of strength A^{77}.

From Eqs. (3.2) and (3.3), it is evident that the slope of a plot of $a(T)$- versus-$\chi_d(T)$, with temperature the implicit parameter, allows the determination of both the sign and magnitude of the corresponding hyperfine interactions. The slope of the straight line of the $a(T)$-versus-χ diagram is given by

$$\partial a/\partial\chi=\alpha'(Ng\beta)^{-1}(A/\gamma\hbar), \qquad (3.4)$$

where $\alpha'=1$ for the Mn^{55} NMR data and $\alpha'=6$ for the Se^{77} NMR data. Equations (3.2) and (3.3) also predict that the resulting straight line of the $a(T)$-versus-χ diagram should pass through the origin. Furthermore, combining Eqs. (3.2) and (3.3) leads to the following expression for α-MnSe

$$a^{77}(T)/a^{55}(T)=6(A^{77}/A^{55})(\gamma^{55}/\gamma^{77}), \qquad (3.5)$$

with a corresponding equation for the ratio of a^{17} to a^{55} in MnO. Thus the slope of an $a^{77}(T)$-versus-$a^{55}(T)$ graph determines the ratio $(6A^{77}/A^{55})$. Equation (3.5) also predicts that the straight line of the $a^{77}(T)$ versus $a^{55}(T)$ graph should pass through the origin. This point is important and will be discussed in greater detail in the sections on MnO and α-MnSe.

MnO

The temperature dependence of the magnetic susceptibility for MnO has been measured by a number of authors.[6–13] Their results for the susceptibility differ as much as 10%; for example, the reported susceptibility maximum at $T\simeq120°K$ varies from about 79 to 84×10^{-6} emu/gram. The Néel temperature of Mno has been established to be $T_N=117\pm1°K$.[14,15]

The O^{17} NMR in the paramagnetic state of MnO has been reported by O'Reilly and Tsang,[16] who found a positive and temperature-dependent O^{17} NMR frequency shift. O'Reilly and Tsang[16] also observed a Lorentzian line shape for the O^{17} NMR with a linewidth $\delta H\simeq4$ Oe. By combining the O^{17} NMR frequency-shift data with magnetic susceptibility measurements, O'Reilly and Tsang[16] calculated an O^{17} transferred hyperfine interaction of strength $A^{17}\simeq+2.4\times10^{-4}$ cm^{-1}.

The measured temperature dependence of the Mn^{55} NMR frequency shift $a^{55}(T)$ in the temperature range of 130 to 350°K is shown in Fig. 2. The solid line shown in Fig. 2, is a smooth curve drawn through the Mn^{55} NMR data. The Mn^{55} NMR frequency shift $a^{55}(T)$ was found to be field-independent between 8 and 16 kOe. At lower magnetic fields, $a^{55}(T)$ could not be determined because of the very large Mn^{55} NMR linewidth $\delta H^{55}\simeq340$ Oe. The data shown in Fig. 2 were taken at a fixed frequency $\nu=16.000$ Mc/sec. Figure 3 shows the result of constructing an $a^{55}(T)$-versus-$\chi(T)$ diagram. The susceptibility data used in Fig. 3 were taken on the same samples for which the NMR measurements were made. As seen in Fig. 3, the graph of

[6] J. J. Banewicz, R. F. Heidelberg, and A. H. Luxem, J. Phys. Chem. **65**, 615 (1961).
[7] J. A. Poulis, C. H. Massen, and P. Van der Leeden, J. Phys. Soc. Japan **17**, Suppl. B-1, 212 (1962).
[8] H. Bizette, B. Squire, and B. Tsai, Compt. Rend. **207**, 449 (1938).
[9] W. D. Johnston and R. R. Heikes, J. Am. Chem. Soc. **78**, 3255 (1956).
[10] T. R. McGuire and R. J. Happel, Jr., J. Phys. Radium **20**, 424 (1959).
[11] S. S. Bhatnager, A. Cameron, E. H. Harbard, P. L. Kapur, A. King, and B. Prakash, J. Chem. Soc. **11**, 1433 (1939).
[12] H. Bizette and B. Tsai, Compt. Rend. **217**, 444 (1943).
[13] R. W. Tyler, Phys. Rev. **44**, 776 (1933).
[14] R. W. Millar, J. Am. Chem. Soc. **50**, 1875 (1928).
[15] S. S. Todd and K. R. Bonnickson, J. Am. Chem. Soc. **73** 3894 (1951).
[16] D. E. O'Reilly and T. Tsang, J. Chem. Phys. **40**, 734 (1964).

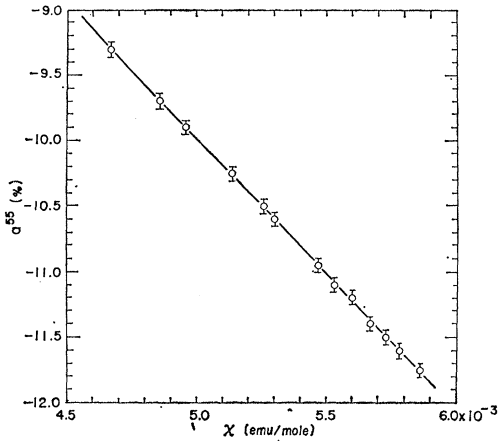

FIG. 3. The Mn^{55} NMR frequency shift $a^{55}(T)$ plotted as a function of the magnetic susceptibility $\chi(T)$ in the paramagnetic state of MnO, with temperature the implicit parameter.

$a^{55}(T)$ versus $\chi(T)$ is a straight line (predicted by Eq. (3.2) and justifies the assumption that the temperature dependence of A^{55} is negligible between 130 and 350°K). The measured slope of the line shown in Fig. 3 is $\partial a^{55}(T)/\partial\chi(T) = -(20.8\pm0.6)$ (emu/mole)$^{-1}$ and yields a value $A^{55} = -(81.5\pm2.2)\times10^{-4}$ cm^{-1} which corresponds to a hyperfine field $H^{55} = -233\pm5$ kOe per unit electron spin. The error estimates for A^{55} were made by finding the maximum and minimum slopes which could be drawn through the data shown in Fig. 3.

The value of the Mn^{55} hyperfine coupling constant A^{55} is to be compared with the value $A^{55} = -(81.2\pm0.05)\times10^{-4}$ cm^{-1} obtained by electron-paramagnetic-resonance (EPR) techniques on the dilute system Mn^{2+}:MgO.[17] Therefore, within experimental error, the hyperfine coupling constant A^{55} for the concentrated system (MnO) is in agreement with the value obtained in the dilute system (Mn^{2+}:MgO). Unfortunately, our experimental measurement of A^{55} in the paramagnetic state of MnO does not have the experimental accuracy needed to detect any small differences in A^{55} between the dilute and concentrated systems. Table I lists various hyperfine coupling constants determined for several sixfold cubic oxygen coordination systems.

TABLE I. Comparison of Mn^{2+} hyperfine coupling for six-fold cubic oxygen coordination.

Lattice	Lattice Constant (Å)	Temperature (°K)	$A^{55}(10^{-4}$ cm$^{-1})$	Reference
MgO	4.203	290	−81.2±0.05	a
		4.2	−81.55	a
CaO	4.797	290	−80.7±0.1	b,c
		77	−81.6	b
		20	−81.7	b
		4.2	−81.7	b
SrO	5.10	290	−78.1±0.2	c
		77	−80.2	c
		4.2	−80.7	c
MnO	4.435	150–300	−81.5±2.2	d
		4.2	−81.51±0.01	e

[a] W. M. Walsh, Jr. (private communication).
[b] W. Low and R. S. Rubins, *Proceedings of the First International Conference on Paramagnetic Resonance*, edited by W. Low (Academic Press Inc., New York, 1963).
[c] A. J. Shuskus, J. Chem. Phys. **41**, 1885 (1964).
[d] This work.
[e] M. E. Lines and E. D. Jones, Phys. Rev. **139**, A1313 (1965).

[17] W. M. Walsh, Jr. (private communication).

Figure 4 shows the complete a^{55}-versus-χ diagram for MnO. The solid-line portion of Fig. 4 represents the data shown in Fig. 3. In Fig. 4, we see that the extrapolated data of Fig. 3 do not intercept the origin as predicted by Eq. (3.2). Including experimental error, the straight line shown in Fig. 4 intercepts the a^{55} axis between 0.1 and 0.8%. There are four possibilities for the nonzero intercept of the a^{55}-versus-χ diagram shown in Fig. 4: (1) There is an error in the value of the Mn^{55} nuclear gyromagnetic ratio of about ½%. (2) There is an orbital contribution to the total magnetic susceptibility, i.e., Van Vleck temperature-independent paramagnetism of the order of $\chi_{VV}\simeq200\times10^{-6}$ emu/mole. (3) The absolute accuracy of the susceptibility measurements is in error by about 3%. (4) There is a small amount of some other phase of the Mn-O system, e.g. MnO_2, present in our samples of MnO, which will contribute to the bulk susceptibility measurements but not to the NMR measurements. We shall present arguments which favor alternative (4) or a combination of (3) and (4).

Since there is no reason at the present time to believe that there may be an error in the value of the Mn^{55} nuclear gyromagnetic ratio, we will not consider this alternative. Let us now consider the possibility of a Van Vleck temperature-independent susceptibility $\chi_{VV}\simeq200\times10^{-6}$ emu/mole. Such a large χ_{VV} implies a fairly large mixing of excited orbital states into the ground state of the Mn^{2+} ion and hence a g value different from $g=2.00$. Electron-paramagnetic resonance-

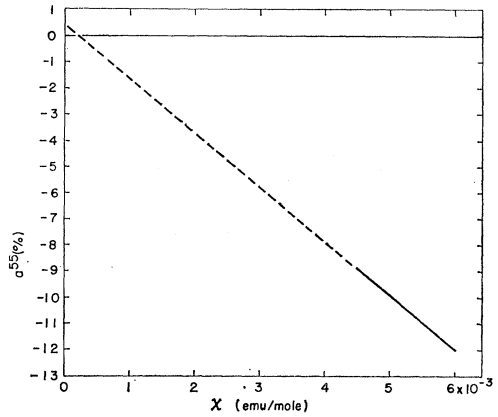

FIG. 4. The complete $a^{55}(T)$ versus $\chi(T)$ diagram for MnO. The solid line in the lower right-hand corner represents the data shown in Fig. 3.

measurements[18] in MnO, however, measure a g value very nearly equal to $g \simeq 2.00$. Thus, on this basis, the probability of a Van Vleck temperature-independent susceptibility seems unlikely.

A method, which eliminates the possibility of Van Vleck temperature-independent paramagnetism is accomplished in the following manner. If there does indeed exist a χ_{VV}, then it is reasonable to assume that it will be due to the Mn^{2+} ion and not the O^{2-} ion. Hence the relationship given by Eq. (3.5) would not be valid, i.e., a plot of a^{17} versus a^{55} will not pass through the origin. In fact, by constructing such a graph, one can determine which ion is the principal contributor to the Van Vleck susceptibility, if it exists in the compound under study. This technique was first utilized by Jaccarino[19] in studying the field dependence of the F^{19} and Co^{59} NMR in the antiferromagnetic state of CoF_2.

Figure 5 shows the result of plotting $a^{17}(T)$ versus $a^{55}(T)$, with temperature the implicit parameter. The O^{17} NMR frequency-shift data are taken from the work of O'Reilly and Tsang.[16] Unfortunately, O'Reilly and Tsang[16] measured $a^{17}(T)$ only at two temperatures and these two data points are shown in Fig. 5. However, we see that we are able to draw a straight line through the data points and the origin. Thus, within the experimental error, the data shown in Fig. 5 indicate that Eq. (3.5) is correct and hence there is no significant Van Vleck temperature-independent susceptibility in MnO. Therefore, we conclude that the nonzero intercept shown in Fig. 4 is probably a result of an absolute error in our susceptibility measurements (about 2%) and/or possibly a small admixture of another Mn-O phase in our samples of MnO. Any small admixture of another Mn-O phase into our samples is probably a result of the method which our samples of MnO were prepared, i.e., converting $MnCO_3$ to MnO at an elevated temperature and hence the possibility of the formation of other oxides of manganese. Furthermore, a small amount (about 3% maximum) of another Mn-O compound or compounds in MnO could not be detected by standard x-ray diffraction techniques.

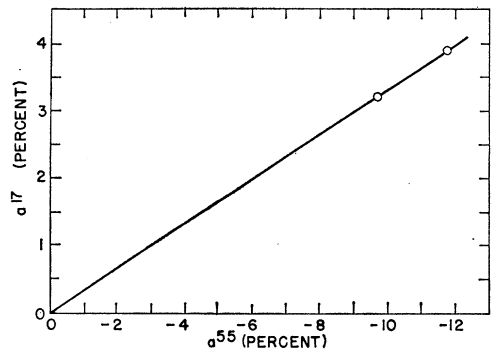

FIG. 5. The O^{17} NMR frequency shift $a^{17}(T)$ data of O'Reilly and Tsang[16] plotted as a function of the Mn^{55} NMR frequency shift $a^{55}(T)$ in MnO with temperature the implicit parameter. The error limits are approximately the size of the open circles.

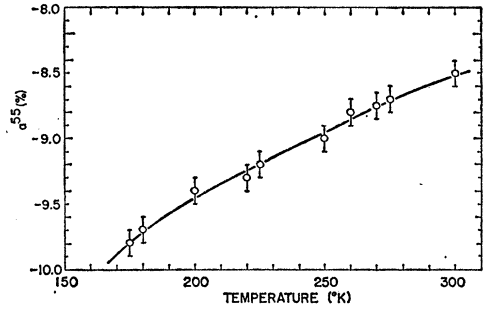

FIG. 6. The temperature dependence of the Mn^{55} NMR frequency shift a^{55} in the paramagnetic state of α-MnS.

The slope of the $a^{17}(T)$-versus-$a^{55}(T)$ diagram shown in Fig. 5 gives the ratio of A^{17} to A^{55}. From Fig. 5, $\partial a^{17}/\partial a^{55} = -0.33$, and from Eq. (3.5),

$$\partial a^{17}(T)/\partial a^{55}(T) = 6(A^{17}/A^{55})(\gamma^{55}/\gamma^{17}). \quad (3.6)$$

Using $A^{55} = -(81.5 \pm 2.2) \times 10^{-4}$ cm^{-1}, Eq. (3.6) yields $A^{17} = +(2.46 \pm 0.05) \times 10^{-4}$ cm^{-1}, in good agreement with the value $A^{17} = +(2.42 \pm 0.04) \times 10^{-4}$ cm^{-1} reported by O'Reilly and Tsang[16] from their O^{17} NMR measurements in the paramagnetic state of MnO. An interesting comparison, which unfortunately cannot be made at the present time, would be to compare the value of the O^{17} hyperfine coupling constant A^{17} obtained from the NMR measurements, with the value obtained by EPR measurements, say in Mn^{2+}:MgO.

α-MnS

Paramagnetic susceptibility measurements[20–22] on α-MnS show a maximum in the region of 155°K while specific-heat measurements by Anderson[23] exhibit an interesting double-cusped curve with one peak at 139°K and the second at 147°K. Our NMR measurements on α-MnS, as discussed below, indicate that the Néel temperature is to be associated with the 147°K peak in the specific-heat data of Anderson.[23]

For the temperature range of 175–300°K, the measured temperature dependence of the Mn^{55} NMR frequency shift $a^{55}(T)$ in α-MnS is shown in Fig. 6. The solid line shown in Fig. 6 is a smooth curve drawn through the Mn^{55} NMR data. The frequency range for which these measurements were taken was 8 to 16 Mc/sec. The Mn^{55} NMR line shape was found to be temperature-independent and Lorentzian with a linewidth $\delta H^{55} \simeq 250$ Oe. There was some indication of line broadening for $T < 170$°K, but the Mn^{55} NMR

[18] L. R. Maxwell and T. R. McGuire, Rev. Mod. Phys. **25**, 279 (1953).
[19] V. Jaccarino (unpublished data).
[20] J. J. Banewicz and R. Lindsay, Phys. Rev. **104**, 318 (1956).
[21] R. Lindsay and J. J. Banewicz, Phys. Rev. **110**, 634 (1958).
[22] J. J. Banewicz, R. F. Heidelberg, and R. Lindsay, Phys. Rev. **117**, 736 (1960).
[23] C. T. Anderson, J. Am. Chem. Soc. **53**, 476 (1931).

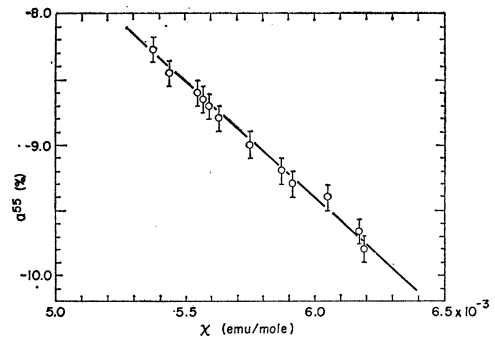

FIG. 7. The Mn^{55} NMR frequency shift $a^{55}(T)$ plotted as a function of the magnetic susceptibility $\chi(T)$ in the paramagnetic state of α-MnS, with temperature the implicit parameter.

signal-to-noise ratio was insufficient to make an accurate determination of this effect.

The Néel temperature for α-MnS was measured by noting the temperature for which the Mn^{55} NMR abruptly disappeared, indicating the onset of antiferromagnetic ordering. The Mn^{55} NMR signal in α-MnS consistently disappeared between 146 and 148°K, thus giving $T_N=147\pm1$°K. This value for the Néel temperature of α-MnS is in agreement with the specific-heat data of Anderson[23] and also with recent susceptibility measurements of Lindsay.[24]

In order to determine the Mn^{55} hyperfine coupling constant A^{55} in the paramagnetic state of α-MnS, we again construct an $a^{55}(T)$-versus-$\chi(T)$ diagram with the result shown in Fig. 7. The slope $\partial a^{55}/\partial\chi$ of the straight line drawn through the data shown in Fig. 7 is $\partial a^{55}/\partial\chi=-18.2$ (emu/mole)$^{-1}$. Thus from Eq. (3.4) and the experimental slope $\partial a^{55}/\partial\chi$, we find $A^{55}=-71.0\times10^{-4}$ cm^{-1} corresponding to a Mn^{55} nuclear hyperfine field $H^{55}=-203$ kOe per unit electron spin.

Extrapolating the data shown in Fig. 7 to zero results in the same difficulty encountered with the analysis of the Mn^{55} NMR frequency-shift data in MnO (see Fig. 4), i.e., the a^{55} versus χ diagram for α-MnS does not pass through the origin as predicted by Eq. (3.2). However, the technique utilized for MnO (plotting the O^{17} NMR frequency shift $a^{17}(T)$ versus the Mn^{55} NMR frequency shift $a^{55}(T)$ as discussed in the section on MnO) cannot be used for α-MnS in order to show that Eq. (3.2) is correct, since the S^{33} NMR in α-MnS has not been observed. The failure to observe the S^{33} NMR in α-MnS is undoubtedly due to the low natural abundance (0.74%) of the S^{33} isotope.

An alternate method of showing that Eq. (3.2) is valid for α-MnS and there are no other contributions to the susceptibility (and thus the Mn^{55} NMR frequency shift a^{55}), is to first rewrite Eq. (3.2) in the following manner:

$$(a^{55}(T)T)^{-1}=(Ng\beta/C)(\gamma^{55}h/A^{55})(1-\theta T^{-1}), \quad (3.7)$$

where we have assumed that between 175 and 300°K, $\chi_d(T)$ can be represented by a Curie-Weiss law, i.e., $\chi_d(T)=C(T-\theta)^{-1}$ with C the Curie-Weiss constant ($C=4.38$ for the Mn^{2+} ion) and θ the Curie-Weiss temperature. Equation (3.7) predicts that a plot of $(a^{55}(T)T)^{-1}$ versus T^{-1} will be a straight line with the slope determining (θ/A^{55}) and the infinite temperature limit giving A^{55} directly. This particular method for analyzing the NMR frequency-shift data is extremely sensitive to any small deviations from Curie-Weiss behavior and has been discussed by Danielian[25] who employed it in analysis of susceptibility data.

Figure 8 is a graph of $(a^{55}(T)T)^{-1}$ versus T^{-1} for α-MnS. The linear relationship between $(a^{55}(T)T)^{-1}$ and T^{-1} shown in Fig. 8 corroborates the assumption of Curie-Weiss behavior for $\chi(T)$ in α-MnS for 175°K $\leq T\leq$300°K. It is interesting to remark that a similar graph for the Mn^{55} NMR data in MnO shows curvature for temperatures approaching the Néel temperature, where the effects of short-range order upon the susceptibility are not negligible.[26] The Mn^{55} NMR frequency shift data in α-MnS for temperatures approaching the Néel temperature could not be measured with sufficient accuracy for us to observe the effects of short-range order. For the higher temperature range, the linear relationship between $(a^{55}(T)T)^{-1}$ and T^{-1} demonstrates, however, that there are no other contributions to $a^{55}(T)$ that need be considered for α-MnS. Therefore the reason for the nonzero intercept in the complete $a^{55}(T)$-versus-$\chi(T)$ diagram for α-MnS is probably the same as was inferred for MnO, i.e., a combination of impure samples and/or an absolute error in the susceptibility measurements.

An analysis of the data presented in Fig. 8 yields $A^{55}=-(71.8\pm5.3)\times10^{-4}$ cm^{-1} and $\theta=-(590\pm60)$°K. This value for A^{55} determined by the data shown in Fig. 8 is in agreement with the value obtained from the a^{55}-versus-χ diagram (Fig. 7). Thus for α-MnS we find a Mn^{55} nuclear hyperfine field $H^{55}=-(205\pm15)$ kOe per unit electron spin. A comparison of sixfold cubic

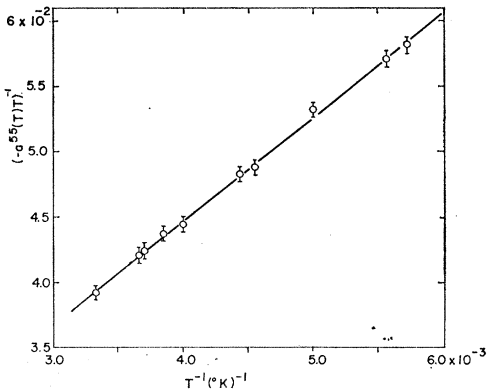

FIG. 8. The quantity $(-a^{55}(T)T)^{-1}$ defined in Eq. (3.7) plotted as a function of T^{-1} for α-MnS.

[24] R. Lindsay (private communication).

[25] A. Danielian, Proc. Phys. Soc. (London) **80**, 981 (1962).

[26] M. E. Lines and E. D. Jones, Phys. Rev. **139**, A1313 (1965).

TABLE II. Comparison of Mn^{2+} hyperfine coupling constants for six-fold cubic sulfur coordination

Lattice	Lattice Constant (Å)	Temperature (°K)	$A^{55}(10^{-4}$ cm$^{-1})$	Reference
MgS	5.19	300	−74.68	a
		77	−74.8	b
		4.2	−75.23	a
CaS	5.68	300	−75.7	c
		77	−76.8	c
SrS	5.87	300	−75.56	a
		77	−76.8	b
		4.2	−77.44	a
α-MnS	5.21	150–300	−71.8±5.3	d
		4.2	−77.72±0.03	e

[a] S. Geschwind (private communication) (estimated accuracy ±0.07 ×10^{-4}cm^{-1}).
[b] P. Auzins, J. W. Orton and J. W. Wentz, *Proceedings of the First International Conference on Paramagnetic Resonance*, edited by W. Low (Academic Press Inc., New York, 1963).
[c] O. Matamura, J. Phys. Soc. Japan **14**, 108 (1958).
[d] This work.
[e] M. E. Lines and E. D. Jones, Phys. Rev. **141**, 525 (1966).

sulfur coordination Mn^{55} hyperfine coupling constants is given in Table II.

α-MnSe

Paramagnetic susceptibility measurements[27–29] on α-MnSe have exhibited a large thermal hysteresis and magnetic field dependence, both of which are dependent upon sample history. This phenomenum has not been observed for MnO or α-MnS. A tentative explanation for this behavior in α-MnSe has been advanced by Lindsay[29] who suggested the possibility of α-MnSe transforming to β-MnSe (zinc blende structure) and/or γ-MnSe (wurtzite structure) as a function of temperature and time. Evidence supporting Lindsay's hypothesis[29] may have been observed by Taylor[30] who measured

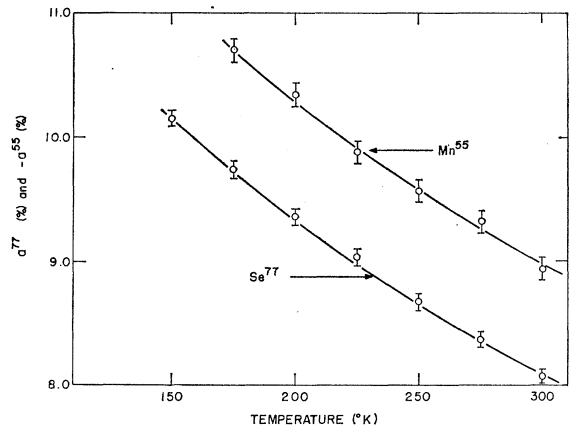

FIG. 9. The temperature dependence of the Mn^{55} and Se^{77} NMR frequency shifts a^{55} and a^{77} for the paramagnetic state of α-MnSe.

[27] H. Bizette and B. Tsai, Compt. Rend. **212**, 75 (1941).
[28] A. Serres, J. Phys. Radium **8**, 146 (1947).
[29] R. Lindsay, Phys. Rev. **84**, 569 (1951).
[30] A. Taylor, Appl. Spectry. **14**, 116 (1960).

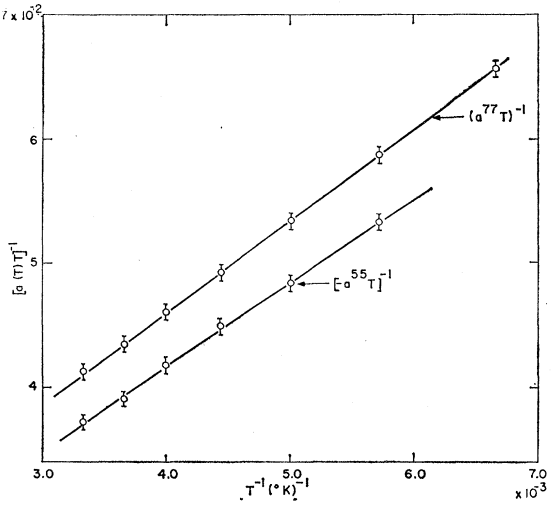

FIG. 10. The quantities $(-a^{55}(T)T)^{-1}$ and $(a^{77}(T)T)^{-1}$ defined by Eqs. (3.8) and (3.9) plotted as a function of T^{-1} for α-MnSe.

lattice constants for α-MnSe as a function of temperature, using x-ray diffraction techniques.

The Mn^{55} and Se^{77} NMR frequency shifts $a^{55}(T)$ and $a^{77}(T)$ have been measured in the paramagnetic state of α-MnSe for the temperature range 150–300°K. The Mn^{55} and Se^{77} NMR line shapes were found to be Lorentzian with the separation between absorption derivative extrema being $\delta H^{55}\simeq 275$ Oe and $\delta H^{77}\simeq 30$ Oe. Figure 9 shows the measured temperature dependence of $-a^{55}(T)$ and $a^{77}(T)$ in the paramagnetic state of α-MnSe. The solid lines shown in Fig. 9 are smooth curves drawn through the Mn^{55} and Se^{77} NMR data. The Mn^{55} NMR disappeared at a temperature $T\simeq 150$°K indicating the onset of antiferromagnetic ordering and hence for α-MnSe, $T_N\simeq 150$°K. This value for T_N is to be compared with susceptibility measurements which indicate $T_N\simeq 285$°K.[27–29]

The measured susceptibility in our samples of α-MnSe exhibited the same type of hysteresis effects mentioned above. On the other hand, the Mn^{55} and Se^{77} NMR frequency-shift data shown in Fig. 9 *did not* exhibit any field-dependent or thermal hysteresis effects over several repeated temperature cycles. Thus, the NMR data are an indication that the observed susceptibility hysteresis is not to be associated with α-MnSe, but perhaps, as Lindsay[29] suggests, the hysteresis is due to conversion of α-MnSe to small amounts of other Mn-Se phases. Since the hyperfine interactions for β- and γ-MnSe will be different than for α-MnSe, we would not observe the NMR for small amounts of β- and γ-MnSe.

Normally, at this point in the analysis of the NMR frequency-shift data, we would determine A^{55} and A^{77} upon constructing $a(T)$-versus-$\chi(T)$ diagrams. However, in contrast to MnO and α-MnS, we do not have any meaningful susceptibility measurements for α-MnSe for which an $a(T)$-versus-$\chi(T)$ diagram can be con-

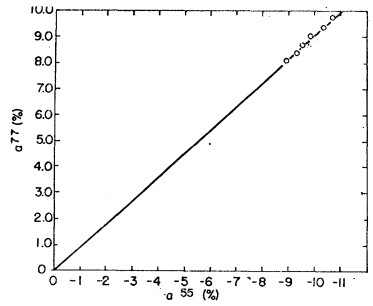

FIG. 11. The Se^{77} NMR frequency shift $a^{77}(T)$ plotted as a function of the Mn^{55} NMR frequency shift $a^{55}(T)$ for α-MnSe, with temperature the implicit parameter. The error limits are approximately the size of the open circles.

structed. We can, however, derive approximate values for A^{55} and A^{77}, using the technique described in the previous section on α-MnS, i.e., Eq. (3.7). For α-MnSe we thus write

$$(a^{55}(T)T)^{-1}=\alpha^{55}(1-\theta T^{-1}), \tag{3.8}$$

and

$$(a^{77}(T)T)=^{-1}\alpha^{77}(1-\theta T^{-1}), \tag{3.9}$$

where

$$\alpha^{55}=(Ng\beta/C)(\gamma^{55}\hbar/A^{55}), \tag{3.10}$$

and

$$\alpha^{77}=(Ng\beta/C)(\gamma^{77}\hbar/6A^{77}) \tag{3.11}$$

with $C=4.38$, the expected Curie-Weiss constant for the Mn^{2+} ion.

The result of plotting $(-a^{55}(T)T)^{-1}$ and $(a^{77}(T)T)^{-1}$ as a function of T^{-1} for α-MnSe is shown in Fig. 10. Figure 10 shows that $(a(T)T)^{-1}$ versus T^{-1} is a straight line for both the Mn^{55} and Se^{77} NMR data and hence, corroborates the assumption of Curie-Weiss behavior for $\chi_d(T)$. An analysis of the data shown in Fig. 10, yields $\theta=-(500\pm50)$°K, $A^{55}=-(67.0\pm4.5)\times10^{-4}$ cm^{-1}, and $A^{77}=+(7.2\pm0.6)\times10^{-4}$ cm^{-1}. The error estimates were made from the maximum and minimum slopes which could be drawn through the data shown in Fig. 10.

A further check upon the above values for A^{55} and A^{77} is furnished by Eq. (3.5), which gives the relationship between $a^{77}(T)$ and $a^{55}(T)$. Figure 11 shows a graph of $a^{77}(T)$ versus $a^{55}(T)$ for α-MnSe with temperature the implicit parameter. It is important to note that a straight line passing through the origin can be drawn through the data. This result indicates that for α-MnSe, there are no contributions to $a(T)$ and/or $\chi(T)$ other than given in Eqs. (3.2) and (3.3) The slope of the straight line shown in Fig. 11 is $\partial a^{77}/\partial a^{55}=-0.90$. Thus, from Eq. (3.6) we find $A^{77}/A^{55}=-0.12$, in good agreement with the ratio $A^{77}/A^{55}=-(0.11\pm0.02)$ obtained from the analysis of the NMR frequency-shift data shown in Fig. 10. The value for A^{55} in α-MnSe determined by the NMR method is in fair agreement with the EPR value $A^{55}=-71\times10^{-4}$ cm^{-1} measured in Mn^{2+}:MgSe.[31]

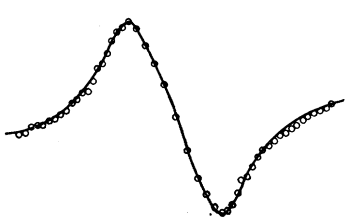

FIG. 12. The Mn^{55} NMR line-shape data (open circles) compared with a calculated Lorentzian (solid line) line shape. The value $(1/T_2)^{55}=1.96\times10^6$ sec^{-1} was used in the calculation for the line shape.

4. NMR LINEWIDTHS IN THE PARAMAGNETIC STATES OF MnO, α-MnS AND α-MnSe

In this section we discuss and interpret the experimentally observed NMR linewidths and line shapes in the paramagnetic states of MnO, α-MnS and α-MnSe.

The observed NMR line shapes in the paramagnetic states of MnO, α-MnS, and α-MnSe were found to be Lorentzian. Figure 12 shows a comparison between a Lorentzian curve (solid line) and experimental points (open circles) for the room-temperature Mn^{55} NMR spectrum in MnO (Fig. 1). The NMR frequency for the data shown in Fig. 12 was $\nu=16$ Mc/sec. Table III lists the corresponding spin-spin relaxation times T_2 for MnO, α-MnS, and α-MnSe where T_2 is given by $(1/T_2)=(\sqrt{3}/2)\gamma\delta H$ with γ the nuclear gyromagnetic ratio and δH the magnetic field separation of the distance between absorption derivative extrema. For purposes of comparison, the second-moment contributions to the NMR linewidths, due to nuclear dipolar interactions, are also presented in Table III. An expression for the second moment $\langle\Delta H^2\rangle$ in a powder sample with the NaCl structure has been given by McGarvey and Gutowsky[32] as

$$(\Delta H^2)_I=(3/5)f_I\gamma_I^2\hbar^2I(I+1)(115.6/a_0^6)+(4/15)f_S\gamma_S^2\hbar^2S(S+1)(422.1/a_0^6), \tag{4.1}$$

where f_I and f_S are the concentrations of the nuclear spins I, and S and a_0 is the lattice constant of the NaCl-type lattice. It is evident from the values of the root-mean-square second moment $\langle\Delta H^2\rangle^{1/2}$ given in Table III that the experimental linewidths are considerably larger than those given by Eq. (4.1).

The theory of exchange-narrowed hyperfine-broadened NMR linewidths in paramagnetic insulators has been treated in detail by Moriya.[1] In the analysis of the NMR data presented in this paper, we make the reasonable assumption that the NMR linewidths in the

TABLE III. The observed NMR linewidths δH in the paramagnetic states of MnO, α-MnS and α-MnSe. The values for $(1/T_2)$ are derived from the expression $(1/T_2)=(\sqrt{3}/2)\gamma H$. Also given, for purpose of comparison, are the root-mean-square second moments $\langle\Delta H^2\rangle^{1/2}$ due to nuclear dipole-dipole interactions.

Compound	δH^{55} (Oe)	δH^{77} (Oe)	$(1/T_2)^{55}$ (10^6 sec^{-1})	$(1/T_2)^{77}$ (10^5 esc^{-1})	$\langle\Delta H^2\rangle_{55}^{1/2}$ (Oe)	$\langle\Delta H^2\rangle_{77}^{1/2}$ (Oe)
α-MnSe	275	30	1.6	1.3	1.1	1.3
α-MnS	250	···	1.44	···	1.2	···
MnO	340	···	1.95	···	1.9	···

[31] O. Matamura, J. Phys. Soc. Japan **14**, 108 (1959).

[32] B. R. McGarvey and H. S. Gutowsky, J. Chem. Phys. **20**, 1472 (1952).

paramagnetic states of MnO, α-MnS and α-MnSe are dominated by an isotropic scalar hyperfine interaction of the form $A\mathbf{I}\cdot\mathbf{S}$. For this type of interaction, Moriya's calculation[1] predicts Lorentzian line shapes (as observed experimentally) and the Mn^{55} T_2 given by

$$(1/T_2)^{55}=[(2\pi)^{1/2}/3](A^{55}/\hbar)^2S(S+1)/\omega_e^{55}, \quad (4.2)$$

with

$$(\omega_e^{55})^2=(2S(S+1)/3\hbar^2)(12J_1^2+6J_2^2), \quad (4.3)$$

where $S=\frac{5}{2}$ is the Mn^{2+} electronic spin, J_1 and J_2 are the corresponding antiferromagnetic exchange interactions for the 12 nearest- and 6 next-nearest-neighboring Mn^{2+} spins.

For the Se^{77} NMR linewidth in the paramagnetic state of α-MnSe, the corresponding expression for the Se^{77} T_2 is

$$(1/T_2)^{77}=6[(2\pi)^{1/2}/3](A^{77}/\hbar)S(S+1)/\omega_e^{77}, \quad (4.4)$$

where

$$(\omega_e^{77})^2=(2S(S+1)/3\hbar^2)(8J_1^2+5J_2^2), \quad (4.5)$$

with a corresponding equation for the O^{17} NMR linewidth in the paramagnetic state of MnO.

The factor of 6 in Eq. (4.4) arises since there are 6 Mn^{2+} ions around a given Se^{77} site, each of which is contributing equally to the Se^{77} NMR linewidth, through the transferred hyperfine interaction A^{77}. The reason for the reduction in the values for the number of nearest and next-nearest neighbors contributing to the exchange-narrowing process for the Se^{77} NMR linewidth i.e., Eq. (4.5), is as follows: Four of the Mn^{2+} electronic spins around each Se^{77} nucleus are nearest neighbors for any given Mn^{2+} spin in this cluster. Since a mutual spin flip (exchange) between any two of these particular Mn^{2+} spins will not affect the value of the Se^{77} nuclear hyperfine field, these Mn^{2+} spins are not to be taken into account in the exchange-narrowing process of the hyperfine-broadened Se^{77} NMR linewidth. However, a mutual spin-flip with another nearest-neighbor Mn^{2+} spin which is not located in the cluster about the Se^{77} nucleus in question, will change the value of the Se^{77} nuclear hyperfine field and hence contribute to the exchange-narrowing process. Thus $z_1=12-4=8$ nearest-neighbor Mn^{2+} spins are to be counted in the exchange-narrowed process. A similar analysis which includes next-nearest-neighbor exchange interactions between the Mn^{2+} spins, gives $z_2=5$.

Since there are no unknown parameters in Eqs. (4.2) through (4.5), we are in a position to calculate values for $(1/T_2)$ and compare the results with the observed $(1/T_2)$ given in Table III.

MnO

Lines and Jones,[26] in their analysis of the magnetic properties of MnO, have determined the exchange energies to be $J_1=10°K$ and $J_2=11°K$. Thus for MnO, from Eqs. (4.3) and (4.5), $\omega_e^{55}=1.38\times10^{13}$ sec^{-1} and $\omega_e^{17}=1.23\times10^{13}$ sec^{-1}. Using $A^{55}=-81\times10^{-4}$ cm^{-1} and $A^{17}=+2.4\times10^{-4}$ cm^{-1}, Eqs. (4.2) and (4.4) give

$$(1/T_2)^{55}=1.23\times10^6 \text{ sec}^{-1}, \quad (4.6)$$

and

$$(1/T_2)^{17}=7.7\times10^3 \text{ sec}^{-1}. \quad (4.7)$$

These calculated values for $(1/T_2)$ are to be compared with the observed $(1/T_2)=1.95\times10^6$ sec^{-1} given in Table III and O'Reilly and Tsang's[16] value $(1/T_2)\simeq1.4\times10^4$ sec^{-1}.

A possible source of error in the calculation for $(1/T_2)$ could be in the definition of ω_e. This error is probably the proportionality constant κ used in the definition of ω_e from $\omega_e^2=\kappa\,\Sigma_i J_i^2$. Several authors[33–35] have used various models to calculate an expression for the exchange frequency ω_e and they differ as much as a factor of 2. Our calculated values for $(1/T_2)$ thus strongly depend upon the value used for the proportionality constant κ.

However, we note from Eqs. (4.2) to (4.4) that

$$(1/T_2)^{17}/(1/T_2)^{55}=6(A^{17}/A^{55})\times\{(12J_1^2+6J_2^2)/(8J_1^2+5J_2^2)\}^{1/2}, \quad (4.8)$$

i.e., the ratio of the $(1/T_2)$'s are independent of the proportionality constant κ. Thus, we see that in order to test Moriya's[1] calculation for MnO, α-MnS and α-MnSe, it is preferable to compare theoretical and experimental values for the ratio's of $(1/T_2)$. From Eq. (4.8), or equivalently, taking the ratio of Eq. (4.7) to (4.6), we calculate

$$(1/T_2)^{17}/(1/T_2)^{55}=6.3\times10^{-3}. \quad (4.9)$$

Thus we see that the calculated ratio given in Eq. (4.9) compares favorably with the observed ratio $(1/T_2)^{17}/(1/T_2)^{55}=7.4\times10^{-3}$.

Since the calculated and observed ratios of $(1/T_2)$ for the O^{17} and Mn^{55} NMR are in good agreement, we feel that the apparent disagreement for the absolute calculation for $(1/T_2)$ in the paramagnetic state of MnO is probably due to the uncertainty of the proportionality constant used in the definition of ω_e.

α-MnS

Values for the exchange energies J_1 and J_2 for α-MnS have been obtained by Lines and Jones[36] with the result $J_1=7°K$ and $J_2=12°K$. For the Mn^{55} NMR linewidth in the paramagnetic state of α-MnS, we calculate $\omega_e=1.2\times10^{13}$ sec^{-1}. Thus we find from Eq. (4.2) and $A^{55}=-71\times10^{-4}$ cm^{-1};

$$(1/T_2)^{55}=1.1\times10^6 \text{ sec}^{-1}, \quad (4.10)$$

in comparison with the observed $(1/T_2)^{55}=1.44\times10^6$ sec^{-1}.

[33] P. W. Anderson and P. R. Weiss, Rev. Mod. Phys. **25**, 269 (1953).
[34] P. W. Anderson, J. Phys. Soc. Japan **9**, 316 (1954).
[35] R. Kubo and K. Tomita, J. Phys. Soc. Japan **9**, 888 (1954).
[36] M. E. Lines and E. D. Jones, Phys. Rev. **141**, 525 (1966).

α-MnSe

In contrast to MnO and α-MnS, there are, presently, no calculations for J_1 and J_2 in α-MnSe. However, since the Néel temperature for α-MnSe is slightly higher than the Néel temperature of α-MnS, we estimate $J_1 \simeq 6°K$ and $J_2 \simeq 13°K$. For α-MnSe, we thus calculate $\omega_e^{55} = 1.2 \times 10^{13}$ sec^{-1} and $\omega_e^{77} = 1.07 \times 10^{13}$ sec^{-1} from Eqs. (4.3) and (4.5). Using the hyperfine interactions $A^{55} = -67 \times 10^{-4}$ cm^{-1} and $A^{77} = +7.2 \times 10^{-4}$ cm^{-1} together with Eqs. (4.2) and (4.4) we find

$$(1/T_2)^{55} = 1.0 \times 10^6 \text{ sec}^{-1}, \tag{4.11}$$

and

$$(1/T_2)^{77} = 7.7 \times 10^4 \text{ sec}^{-1}. \tag{4.12}$$

Comparing Eqs. (4.11) and (4.12) with the observed $(1/T_2)^{55} = 1.6 \times 10^6$ sec^{-1} and $(1/T_2)^{77} = 1.3 \times 10^5$ sec^{-1} we again see that, as was the case with MnO and α-MnS, there is a fairly large discrepancy between theory and experiment.

However the calculated ratio of $(1/T_2)^{77}$ to $(1/T_2)^{55}$ of

$$(1/T_2)^{77}/(1/T_2)^{55} = 7.7 \times 10^{-2}, \tag{4.13}$$

is in good agreement with the experimental ratio $(1/T_2)^{77}/(1/T_2)^{55} = 8.3 \times 10^2$ for α-MnSe. Of course, the ratio given by Eq. (4.13) is rather insensitive to small errors in the values for J_1 and J_2 in α-MnSe, while the absolute calculation for $(1/T_2)$ given by Eqs. (4.2) or (4.4) are not as insensitive to errors in J_1 and J_2.

Therefore, for MnO, α-MnS and α-MnSe, we find that Moriya's[1] calculation for the effects of exchange-narrowing upon NMR linewidths in paramagnetic insulators is in good agreement with experiment. Other contributions to the NMR linewidth, which Moriya[1] considers, such as the effect of fluctuations of the dipolar field due to the Mn^{2+} electronic spins etc., have been neglected in the preceding calculations for the NMR linewidths. Since the calculated and observed ratios of the NMR linewidths are in good agreement, we conclude that other contributions to the NMR linewidth are small.

5. SUMMARY

We have presented and discussed the observation of the Mn^{55} NMR in the paramagnetic states of MnO, α-MnS and the Mn^{55} and Se^{77} NMR in the paramagnetic state of α-MnSe. An analysis of the NMR frequency-shift data yielded information regarding the magnitude and sign of the hyperfine interactions present in these compounds. It was shown that the principal contribution to the Mn^{55} nuclear hyperfine interaction was due to the negative core-polarization term, while other interactions resulting from Van Vleck temperature-independent susceptibilities, etc. are small, if even present. The technique used to demonstrate the preceding conclusion for α-MnS and α-MnSe made use of a novel technique for analyzing the NMR data, i.e., plotting $(a(T)T)^{-1}$ versus T^{-1} which is a variant of the method suggested by Danielian[25] for analysis of susceptibility data.

The values for the Mn^{55} nuclear hyperfine interactions determined for MnO, α-MnS and α-MnSe were found to be within experimental error with the values obtained by the EPR method on the dilute Mn^{2+} systems. Unfortunately, the experimental accuracy of the NMR measurements in the concentrated magnetic systems was not sufficient to be able to make quantitive conclusions regarding small differences in the hyperfine field between the dilute and concentrated systems.

Other information, such as the Néel temperatures of α-MnS and α-MnSe, was obtained by studying the temperature dependence of the Mn^{55} NMR signal, with the result $T_N(\alpha\text{-MnS}) = 147 \pm 1°K$ and $T_N(\alpha\text{-MnSe}) \simeq 150°K$.

The result of applying the theory[1] of exchange-narrowed hyperfine-broadened NMR in paramagnetic insulators was shown to be in good agreement with experiment. This agreement did not manifest itself in the calculation for the individual NMR linewidths but rather in the calculation in the ratios of the NMR linewidths between two nuclear species present in the same compound, e.g., Mn^{55} and Se^{77} in α-MnSe.

ACKNOWLEDGMENTS

The author is grateful fo Dr. V. Jaccarino and Professor P. Pincus for several helpful discussions concerning the theory of NMR in paramagnetic materials and to R. C. Sherwood for performing the susceptibility measurements.